The Impact of Intercontact Time within Opportunistic Networks: Protocol Implications and Mobility Models

Muhammad Abdulla and Robert Simon
Department of Computer Science
George Mason University
Fairfax, VA 22030
Email: {mabdulla, simon}@cs.gmu.edu

***Abstract*—Opportunistic networking, where node mobility is utilized to achieve message delivery, has become an important class of mobile ad hoc networking. A critical component of performance analysis for opportunistic networking is a basic understanding of contact and inter-contact times for commonly studied mobility models. In this paper we give original results nodal contact-times and analytically show that inter-contact times of mobile nodes can be closely approximated as exponentially distributed in Random Waypoint and Random Direction mobility models. We then examine the effect of $HELLO$ intervals on the observed inter-contact rate of nodes. Through extensive simulation study, we show that our analytical results for mobility characteristics are accurate.**

I. Introduction

Routing schemes for traditional mobile ad hoc networks (MANETs) assume that nodes are well connected most of the time. Generally, proactive schemes, where nodes try to keep up to date routing information [24], or reactive schemes, where nodes find routing paths on demand [17, 25], are used to achieve message delivery. Both schemes assume that there exists an end-to-end path from source to destination at the time of message transfer. However, such assumptions do not hold true when the mobile network is sparse and is intermittently connected.

Routing methods for such sparse mobile networks use a different paradigm for message delivery; these schemes utilize node mobility by having nodes carry messages, waiting for an opportunity to transfer messages to the destination or the next relay rather than transmitting them over a path [15, 26, 29, 30, 35]. Opportunistic networking (ON), where node mobility is utilized to achieve message delivery, has become an important class of mobile ad hoc networking. Under such opportunistic network routing protocols [31], nodes forward messages only when they encounter the appropriate relay or the destination node. Due to this dependence on mobility, understanding mobility characteristics such as inter-contact times of mobile nodes within each other or at a static location plays an important role in the design and analysis of routing algorithms under this paradigm.

In this paper we first give analytical results for node contact times when two nodes come into contact with each other. This is an important parameter in mobility-assisted networks as contact times represent the duration of message communication opportunity upon a contact. We then analytically show that nodal inter-contact times can be closely approximated as exponentially distributed under Random Waypoint (RWP) and Random Direction (RD) mobility models. This is important in understanding the performance of routing schemes for opportunistic networks, as the inter-contact times of nodes are the major component of message delay. Understanding the rate and exponentiality characteristics of inter-contact times under RWP and RD models is useful in two aspects. Firstly, it allows the experimenter to use these models when it is assumed that the underlying mobility has exponential inter-contact times. Secondly, it enables the analysis and explanation of performance measurements based on the exponentiality characteristics when these mobility models are used in experiments. For inter-contact times, we extend our results further by considering the effect of beaconing ($HELLO$) messages on the observed inter-contact rate. This result is important in understanding the trade-offs when tuning beaconing intervals, since larger $HELLO$ intervals decrease energy usage, while increasing inter-contact times, contributing to larger message delays. Through extensive simulation study, we show that our analytical results for mobility characteristics are accurate.

The rest of the paper is organized as follows. Section II goes over the background and related work. Section III discusses the stochastic mobility properties of the Random Waypoint and Random Direction mobility models. Section V presents experimental results. Finally, Section VI concludes the paper.

II. Background and Related Work

Mobility models play an important role in the simulation study of mobile networks. Two common mobility models are the Random Waypoint (RWP) and Random Direction (RD). Other mobility models are proposed by different groups [1, 6, 9, 10, 31]. Also, issues such as non-uniform node distribution and speed decay have been addressed for the RWP model [3, 33]. However, RWP and RD mobility models are currently widely used in network simulations and are the focus of

our study. Before we continue our discussion we go over background, assumptions, and related work.

A. Background

In this study, we focus on two epoch-based mobility models: Random Waypoint (RWP) and Random Direction (RD). For practical purposes, we consider a two-dimensional system space $\mathcal{A}$ of size A as a square area of width a or a circular region with radius a. The movement of a node from a starting position to its next destination is denoted as a *movement epoch*, or an *epoch* in short. In epoch-based mobility schemes, a node starts from point $P_i \in \mathcal{A}$, and moves to another point $P_{i+1} \in \mathcal{A}$ according to the movement semantics of the mobility model to complete the epoch. It then pauses for a random amount of time T_p, randomly chosen with the expected value of $\bar{T}_{pause}$. This process repeats in this manner. We use $\bar{L}$ to denote average epoch distance, and use $\bar{T}$ to denote average epoch duration. The movement speed v is uniformly and randomly chosen from $[v_{min}, v_{max}]$, where $0 < v_{min} < v_{max} < \infty$.

Formally, Random Waypoint can be specified as a stochastic process

$$\{P_i, T_{p,i}, V_i\}_{i\in\mathbb{N}} = \{(P_1, T_{p,1}, V_1), (P_2, T_{p,2}, V_2), \cdots\}$$

where $T_{p,i}$ is the pause time at waypoint P_i, and V_i is the velocity of node during the i^{th} epoch. P_i is assumed to be independently and identically distributed (i.i.d) at random, uniformly chosen from $\mathcal{A}$. Due to ergodicity properties of movement and distribution under RWP [2], the average epoch length for a convex area $\mathcal{A}$ is given by

$$\bar{L} = \frac{1}{A^2}\int_{\mathcal{A}}\int_{\mathcal{A}} \|P_1 - P_2\| dP_1 dP_2 \tag{1}$$

where $\|P_1 - P_2\|$ is the distance between waypoints P_1 and P_2. That is, the analysis of stochastic properties under RWP model can be simplified by only considering two independent points randomly chosen from system area. For a square area of size $a \times a$, we have $\bar{L} = 0.5214a$, and for a circle of radius a, we have $\bar{L} = 0.9054a$ [2].

Similarly, the Random Direction can be specified as a stochastic process

$$\{T_i, T_{p,i}, V_i\}_{i\in\mathbb{N}} = \{(T_1, T_{p,1}, V_1), (T_2, T_{p,2}, V_2), \cdots\}$$

where T_i is the duration of i^{th} epoch, and is randomly generated from an exponential distribution with an average of $\bar{T} = \bar{L}/\bar{v}$. As in RWP, $T_{p,i}$ is the pause time before the i^{th} epoch starts. V_i denotes the velocity at the start of epoch i, and may change its direction if the border is reached before T_i elapses.

Although movement direction may change during an epoch, as in the case of Random Direction with reflection, we assume the speed remains the same in an epoch. The average node speed, $\bar{v}$, is defined as

$$\bar{v} = \frac{\bar{L}}{\bar{T}}$$

The expected aggregate node speed, v^*, when considering pause times is given as

$$v^* = \frac{\bar{L}}{\bar{T} + \bar{T}_{pause}} \tag{2}$$

Nodes are assumed to have circular radio range with radius r. For the case of sparse mobile networks, we assume that $r \ll a$ and that $r \ll \bar{L}$.

B. Related Work

The stochastic properties of the Random Waypoint mobility model have been extensively studied [2, 3, 20, 23]. Similar studies are also available for the Random Direction model [4, 5, 22]. Most of these studies focus on node distributions, epoch lengths, and movement directions, and are a foundation for further analysis of node movement characteristics under the mobility models. Analytical results for transient behavior of nodes under RWP and RD are presented in [12]. Modeling of steady-state and transient behaviors of user mobility based on real world traces are discussed in [21]. Results for the expected *hitting time* and *meeting time* in RWP and RD models are given in [31] in the context of mobility-assisted routing. Similar results are presented in [13] for the analysis of message delay under sparse networks.

In our study, we focus on the rate and the distribution of inter-contact times under RWP and RD models. This is because the inter-contact time is the main contributing factor to message delays as the effects of the contact time and the message transfer time are comparatively small under typical opportunistic network conditions. To analyze inter-contact times we first view node activities as interleaving encounters and departures—nodes spend some time within each other's radio range after a contact, and spend some more time before they encounter each other again. We show analytically that inter-contact times in RWP and RD models can be closely approximated by an exponential distribution and provide analytical and experimental results. Further, since message transfers only occur when nodes meet each other, we also discuss the contact time of nodes when they come into contact. We also discuss the effects of *hello intervals* on the observed inter-contact rate.

The near-exponential distribution of inter-contact times in RWP and RD models surfaces in different experimental studies [13, 32]. In [13], authors analyze the message delay in epidemic routing under the assumption that the inter-contact times are exponentially distributed, and experimentally verify the validity of the assumption under Random Waypoint and Random Direction models. Based on this exponentiality assumption, further modeling of Epidemic routing performance is provided in [34]. Many studies also use Markovian model for node inter-contact times with or without assuming RWP or RD mobility model [27–29, 32]. Unlike this earlier work, we show that the inter-contact times can be approximated as exponentially distributed. This helps to simplify the analysis of routing schemes under RWP or RD models, and to relate experimental results to analytical models. It also enables us to

use these two mobility models for simulation when the inter-contact times are known to be exponentially distributed.

Understanding the movement characteristics of common mobility models and performance analysis are important in the understanding and evaluation of MANET routing schemes. We believe that our analysis of mobility characteristics and performance metrics will be helpful in the analysis and design of various opportunistic routing schemes for intermittently connected mobile networks.

III. Stochastic Properties of Mobility Models

In this section, we study the statistical properties of node encounters, focusing on node inter-contact times and contact times using two commonly used mobility models: Random Waypoint (RWP) and Random Direction (RD). Within node inter-contact times, we look at inter-contact times between two mobile nodes and inter-contact times of a mobile to a static location.

From the viewpoint of a mobility model, node movements consist of interleaving periods of movements and pauses. From an application's point of view, node N sees the movements of another node M in terms of the time that M spends in its radio range, which we call as *contact time*, and the *inter-contact time* between two contacts. The contact time is defined as the time elapsed from a node's entry into another node's radio range until its consequent exit. The inter-contact time is defined as the time passed since previous exit until next entry into the radio range.

In this section, we first provide analytical results for node contact times. We then analytically show that nodal inter-contact times under RWP and RD mobility models can be closely approximated as exponentially distributed under basic assumptions. Further, we provide analytical results for relative speeds of mobile nodes for the two mobility models, which are necessary to calculate the inter-contact rates and are helpful in explaining the differences in inter-contact rates of RWP and RD mobility models.

A. Contact Times

As discussed above, the contact time is one of the two important aspects of node mobility from the viewpoint of an application. It provides an estimate of the expected time two nodes will have for message exchange when they come into contact.

In terms of movement behavior upon entering the radio range of another node, there are no fundamental differences between RWP and RD mobility models, especially when $r \ll \bar{L}$. Hence, we do not discriminate between the two models in our analysis of contact times.

Figure 1 depicts the scenario where node M is moving into the radio range of node N at velocity $\overrightarrow{v}$. We take the position, P_N of node N as the center of the coordinate system and the direction of M's velocity $\overrightarrow{v}$ to be the direction of x-axis. Here we assume that the PDF of a mobile node crossing the y-axis at a point y is uniform in the range $(-r, r)$. This is reasonable as we assume that $r \ll a$. This assumption is different from [16]

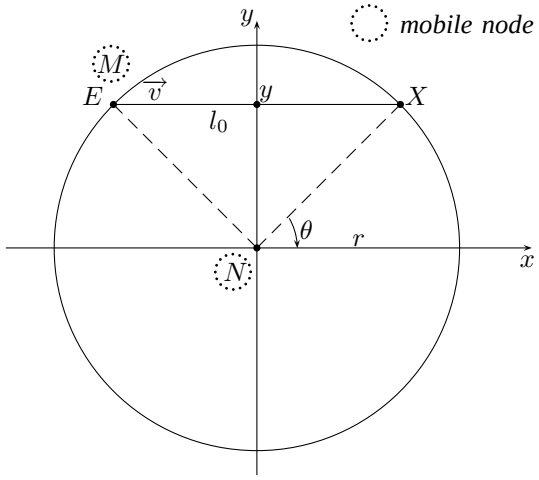

Fig. 1. Calculation of Contact Time

where the direction from M to N is taken as the direction of x-axis and the movement angle measured from x-axis is assumed to be uniform. We note that our result for the contact time is consequently different from the result given in [16]. We empirically validate our results in Section V.

Theorem 1: Let r be the radius of radio range and let a be the radius of system area. Under the assumption that $r \ll a$, the expected contact time, $\bar{T}_C$, of a static node and a mobile node is given as:

$$\bar{T}_C = \frac{\pi r}{2v^*}$$

where v^* is the expected aggregate speed given in Equation (2).

Proof: We first examine the case where there is no epoch change while M covers the distance, l_0, from E to X. We then extend our result by considering the case where an epoch change occurs before M exits the radio range of N.

To calculate l_0, we introduce two auxiliary segments NX and NE as shown in the figure. We use y to denote the intersection of EX and y-axis. It is easy to see that

$$l_0 = \|EX\| = 2r\cos\theta = 2\sqrt{r^2 - y^2}$$

Since the intersection point y can occur anywhere in the range of $(-r, r)$, the expected distance covered within the circle, $\bar{l}_0$, can be given as follows:

$$\bar{l}_0 = \frac{1}{2r}\int_{-r}^{r} 2\sqrt{r^2 - y^2}dy = \frac{\pi r}{2} \tag{3}$$

The result above is obtained under the assumption that $\overrightarrow{v}$ does not change within the radio range. Given r is small compared to $\bar{L}$, we can ignore the probability of two or more direction changes, and only consider the case where one direction change may occur, the probability for which, P_c, can be estimated as

$$P_c = \frac{\bar{l}_0}{\bar{L}}$$

The expected distance covered in the circle before the change occurs is $\bar{l}_0/2$. We have calculated that the expected distance covered before node exits the radio circle from the pause location is approximately $0.9r$ (see Appendix). Therefore, the expected distance that M covers before exiting the circle is:

$$\begin{aligned}\bar{l} &= \bar{l}_0(1-P_c) + P_c(\frac{\bar{l}_0}{2} + 0.9r) \\ &= \bar{l}_0 + \frac{P_c}{2\pi}(3.6-\pi)\bar{l}_0 \\ &\approx \bar{l}_0\end{aligned}$$

The approximation holds true as $P_c = \bar{l}_0/\bar{L}$ is small compared to 1, and $P_c(3.6-\pi)/2\pi \approx 0.07P_c \ll 1$.

Since the average pause between two epochs is $\bar{T}_{pause}$, the expected time spent in the radio range, $\bar{T}_C$, can be expressed as follows:

$$\begin{aligned}\bar{T}_C &= \frac{\bar{l}}{\bar{v}} + P_c\bar{T}_{pause} \\ &\approx \frac{\bar{l}_0}{\bar{v}} + \frac{\bar{l}_0}{\bar{L}}\bar{T}_{pause} \\ &= \bar{l}_0(\frac{\bar{T}+\bar{T}_{pause}}{\bar{L}}) \\ &= \frac{\pi r}{2v^*} \end{aligned} \quad (4)$$

A simplification of the expression is made above by applying the definition of the aggregate speed v^* as given in Equation (2). ■

When both nodes are mobile, relative speed $\tilde{v}$, which we discuss below, is used instead of $\bar{v}$ in the calculation of $\bar{T}_C$.

B. Inter-contact Times in Random Waypoint Model

We first show that after reaching stationary distribution, the contact times of mobile nodes at a static location can be closely approximated as exponentially distributed, and show that result also holds true for inter-contact times under our assumptions regarding the network. We use the expected speed, $\bar{v}$, in our calculations, and the aggregate speed, v^* can be used if pause times need to be considered.

1) Inter-contact Times of a Mobile and a Static Node: Due to i.i.d. property of node movements in RWP, we only have to consider the mobility of a single node. Given that the PDF $f(x,y)$ denotes the probability density of node distribution of mobile node M at position (x,y), the probability, p, of M going through the radio range of N in an epoch is approximated as follows [14, 31]:

$$p = 2r\bar{L}f(x,y) \quad (5)$$

This is because M can cross anywhere in the segment $(-r,r)$ of length $2r$ in the y-axis, as shown in Figure 1, during an epoch. Here $f(x,y)$ is used to approximate the PDF of node distribution within the radio range, which is reasonable under the assumption that $r \ll a$. Although two consecutive epochs are not independent due to the overlap of end-points, we can view epochs in RWP model as independent as shown in [2] due to ergodicity, and the inter-contact times can be described using a geometric distribution in terms of epochs:

$$P(N_{hit} > n) = (1-p)^n = \left(1 - 2r\bar{L}f(x,y)\right)^n \quad (6)$$

Here N_{hit} denotes the epoch that M comes into contact with N, and $P(N_{hit} > n)$ denotes probability that M has not encountered N till after n epochs. This result is given in [31] as *hitting time* of a mobile node at a random location at a static position at (x,y), assuming that M starts its movement at a random location at time 0.

Since the node movement in one epoch continues in the same direction till the end of an epoch, and we cannot extend the results above for arbitrarily small time intervals as the independence assumption does not hold within an epoch, contrary to the argument in [14]. Further, for inter-contact time we have to consider that once two nodes come into contact, the position of the mobile node can no longer be considered random as the next inter-contact time is calculated from the time when the mobile node exits the radio range. Below we discuss factors affecting nodal inter-contact times after a contact, and show that hitting times and inter-contact times above $1.5\bar{T}$ can be closely approximated as exponential using analytical results.

As discussed above, mobile node M spends some time with the radio range of node N and eventually moves out. The expected distance between N and M when M pauses and chooses a new speed and direction can be approximated as $\bar{L}/2$. We know from Equation (1) that $\bar{L}$ denotes the expected distance between two endpoints in the stationary distribution of RWP. On one hand, this means M starts a new epoch at a closer location than the average case in stationary distribution. Intuitively, it can be expected that this decreases the inter-contact time. Further, as given in [2] the mobile node is more likely to choose a direction in the opposite direction, which also increases the likelihood of crossing the radio range of the static node. On the other hand, the expected contact-time increases since M is expected to continue its movement away from N for a distance $\bar{L}/2$, for a total round-trip distance of $\bar{L}$, or a round-trip time of $\bar{T}$. In other words, inter-contact times smaller than $\bar{T}$ have lower likelihood of happening.

If the node M chooses a random waypoint such that it does not cross the radio range of the static node, it will be at a totally independent position after covering $\bar{L}$ in an expected time of $\bar{T}$. Under this condition, the expected time to reach the new waypoint is $1.5\bar{T}$. Although we can see from the analysis above that the inter-contact times cannot be modeled as exponential, when the average epoch time, $\bar{T}$, is much smaller than the expected inter-contact time, $\bar{T}_{ic}$, the geometric distribution given in Equation (6) can be closely approximated as exponential. For this, we give the following lemma:

Lemma 1: Let r be the radio range radius, let a be the radius of the system area, let $\bar{T}$ be the expected epoch duration, and let $\bar{T}_{ic}$ be the expected hitting time. Assuming $r \ll a$, then $\bar{T}/\bar{T}_{ic} = p \ll 1$ holds true.

Proof:

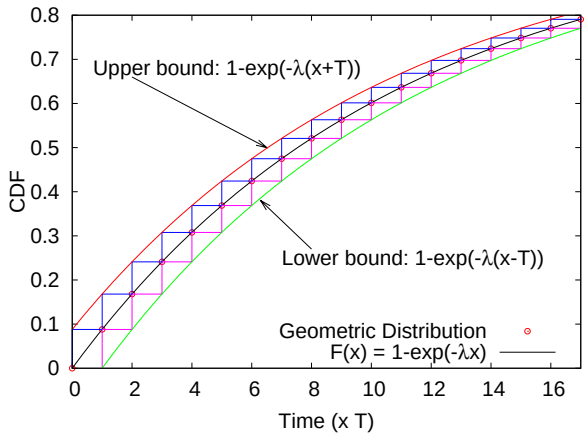

Fig. 2. Exponential Bounds for Geometric Distributions

Since the hitting time can be described as geometric distribution as described in Equation (6), the expected hitting time is given as $\bar{T}_{ic} = \bar{T}/p$. Without loss generality we assume that $f(x,y) = 1/a^2$ to obtain the following:

$$\frac{\bar{T}}{\bar{T}_{ic}} = p = 2r\bar{L}f(x,y) = \frac{2\bar{L}r}{a^2} \approx \frac{r}{a}$$

As $r \ll a$, the assumption that $\bar{T}/\bar{T}_{ic} = p \ll 1$ holds. Similar result can be obtained for circular regions.

■

Although the geometric distribution is used to describe the node inter-contact times in terms of the number of epochs, nodes can come into contact at any time during an epoch. We use $F(t)$ for CDF of inter-contact times in continuous time domain. With the theorem given below we quantify the bounds of exponential approximation of hitting times and inter-contact times using an exponential distribution with a rate of $\lambda = -\ln(1-p)/\bar{T}$, where we use $F_x(t)$ to denote the CDF of the approximating exponential distribution.

Theorem 2: Let r be the radius of radio range, let a be the radius of system area, let $\bar{T}$ be the expected epoch duration, let $\bar{v}$ be the expected speed of a mobile node, and let $f(x,y)$ be the PDF of node distribution at position (x,y). Further, define $\mathbf{I}_s$ as interval $[1.5\bar{T}, \infty)$. Assuming $r \ll a$, the distribution inter-contact times $t \in \mathbf{I}_s$ can be closely approximated as exponentially distributed satisfying the following condition

$$\sup_{t \in [1.5\bar{T}, \infty)} |F_x(t) - F(t)| \leq p$$

where p is given by Equation (5), and satisfies the condition $p \ll 1$ as given in Lemma 1.

Proof:

As discussed above, hitting times and inter-contact times larger than $1.5\bar{T}$ can be described using a geometric distribution as given in Equation (6). We introduce two geometric distributions $F_g^u(i) = 1-(1-p)^{i+1}$ and $F_g^l(i) = 1-(1-p)^i$, for upper and lower bounds of the CDF, $F(t)$, respectively. Since any CDF is monotically increasing, regardless of the shape of $F(t)$ between point $(i, 1-(1-p)^i)$ and point $(i+1, 1-(1-p)^{i+1})$ for $i = 0, 1, \ldots$, the CDF is totally contained within the rectangular region bounded by the CDFs of two bounding geometric distributions: $F_g^u(i)$ and $F_g^l(i)$, as shown in Figure 2. Further, we bound $F_g^u(i)$ and $F_g^l(i)$ using two exponential CDFs, $F_x^u(t) = 1 - e^{-\lambda(t+\bar{T})}$ and $F_x^l(t) = 1 - e^{-\lambda(t-\bar{T})}$, respectively. Since $\lambda = -\ln(1-p)/\bar{T}$ the following holds true for $i = 0, 1, \ldots$:

$$F_x^u(i \times \bar{T}) = 1 - e^{-\lambda(i+1)\bar{T}} = 1 - (1-p)^{i+1} = F_g^u(i)$$

Considering that the result above and the fact that $F_g^u(i)$ is constant in time interval $[i\bar{T}, (i+1)\bar{T})$, and $F_x^u(t)$ is strictly monotically increasing during the same interval, we can see that $F_g^u(i)$ is upper bounded by $F_x^u(t)$ for $t > 0$. Using similar analysis we can show that $F_g^l(i)$ is lower bounded by $F_x^l(t)$ for $t > \bar{T}$, as shown in Figure 2.

As given above, the CDF of the inter-contact times, $F(t)$, is upper- and lower-bounded by $F_x^u(t)$ and $F_x^l(t)$, respectively. It is not hard derive that $F_u(t) - F(t)$ is monotically decreasing:

$$\frac{d(F_u(t) - F(t))}{dt} = \lambda(e^{-\lambda(t+\bar{T})} - e^{-\lambda t}) < 0, \quad 0 \leq t$$

and has the largest value of $(F_u(t) - F(t))|_{t=0} = 1 - e^{-\lambda\bar{T}} - (1 - e^0) = p$ at $t = 0$. It can be similarly obtained for the $F(t) - F_l(t)$ is monotically decreasing for $t > \bar{T}$ and has the largest value at $(F(t) - F_l(t))|_{t=\bar{T}} = 1 - e^{-\lambda\bar{T}} - (1 - e^0) = p$ at time $t = \bar{T}$. This completes the required proof.

■

The implications of the theorem above are that inter-contact times can be closely approximated as exponential except for a small interval $[0, 1.5\bar{T}]$, as $\bar{T} \ll \bar{T}_{ic}$. Using the same reasoning above, hitting times can be also shown to follow the same bounds. We can also see that since $p \ll 1$, the bounds also tight. Further, the geometric distributions used as upper- and lower-bounds above corresponds to the assumptions that node contacts only occur at the beginning of an epoch or at the end of an epoch, respectively. Since the probability of coming into contact with the static node during an epoch can be considered uniformly distributed within the epoch without any specific assumptions, the CDF of inter-contact times can be expected to be much closer to that of the approximating exponential distribution, and the the upper and lower bounds can also be expected to much tighter than the results given above.

2) Inter-contact Times of Two Mobile Nodes:

Theorem 3: Let r be the radius of radio range, let a be the radius of system area, let $\bar{T}$ be the expected epoch duration, let $\bar{v}$ be the expected speed of a mobile node and let $f(x,y)$ be the PDF of node distribution at position (x,y). Further, define $\mathbf{I}_s$ as interval $[1.5\bar{T}, \infty)$. Assuming $r \ll a$, the distribution of inter-contact times of two mobile nodes in $t \in \mathbf{I}_s$ can be closely approximated as exponentially distributed satisfying

the following condition:

$$\sup_{t\in[1.5\bar{T},\infty)} |F_x(t) - F(t)| \leq p$$

where $p = 2r\rho\bar{L}/A$, in which $\rho = A\iint f^2(x,y)dxdy$. Further, $F(t)$ is the CDF of inter-contact times, and $F_x(t)$ is the CDF of approximating exponential distribution with rate $\lambda = -\ln(1-p)/\bar{T}$.

Proof: The proof for the inter-contact rate for two mobile nodes are mostly similar to Theorem 2 above, except for the calculation of inter-contact rate is are discussed below, and is thus omitted. ■

The inter-contact time of two mobile nodes is given as the expected *meeting time* in [31]. Under the simplifying condition that $T_{pause} = 0$, the expected meeting time given in [31] can be written as:

$$EM_{rwp} = \frac{A}{2r\hat{v}_{rwp}\bar{v}} = \frac{A}{2r\tilde{v}}$$

where $\hat{v}_{rwp}$ is the normalized relative speed for RWP, which is calculated to be 1.754 in [31] when the speed of both mobile nodes is set to $\bar{v}$, compared to $\hat{v}_{rd} = 1.27$ for the Random Direction model. We can get the expected meeting rate, λ_{rwp}, according to the expression above as $\lambda_{rwp} = 2\tilde{v}r/A$. The differences in the $\hat{v}_{rwp}$ and $\hat{v}_{rd}$ is attributed to the non-uniformity of movement direction at the beginning of an epoch under the Random Waypoint model, which has a strong bias towards the center [2, 31].

We argue that, due to circular symmetry in a circular area, the non-uniformity of movement direction at the beginning of an epoch under Random Waypoint model does not contribute to the differences between the normalized speeds of Random Waypoint and Random Direction models. The differences of between the differences in the inter-contact rates of the two models is due to the factor $\rho = A\iint f^2(x,y)dxdy$, which is defined by the system area $\mathcal{A}$, and the differences in the distribution of nodal speed, even with the same pair of v_{min} and v_{max} for both models. To show this, we first prove that the relative movement angle of the two mobile nodes is uniformly distributed under RWP in a circular region. We then calculate the ρ values for circular and square regions. We also provide expressions for the calculation of relative movement speeds for both Random Waypoint and Random Direction models.

Theorem 4: Let A and B be two mobile nodes in a circular region moving according to the Random Waypoint mobility model, then the relative movement angle, $\theta_{v_{AB}}$, between their velocities is uniformly distributed. That is:

$$f_{\Theta_{V_{AB}}}(\theta_{v_{AB}}) = \frac{1}{2\pi}, \quad \theta_{v_{AB}} \in [0, 2\pi)$$

where $f_{\Theta_{V_{AB}}}(\theta_{v_{AB}})$ is the PDF of relative movement angle distribution.

Proof: Let us assume that node A is at an arbitrary locations inside the circular region of radius a. For simplicity let us take the center of the circular region, O, as the origin of the polar coordinate system, and take the direction from O to the location of node A as the direction of polar axis, as shown Figure 3. Node A's movement angle, θ_{v_A} is calculated from line OA in counter-clockwise direction. Similarly, assuming node B's coordinate is (r_B, θ_B), node B's movement angle, θ_{v_B} is calculated from line OB in counter-clockwise direction. It is easy to see from Figure 3 that the following relationship holds:

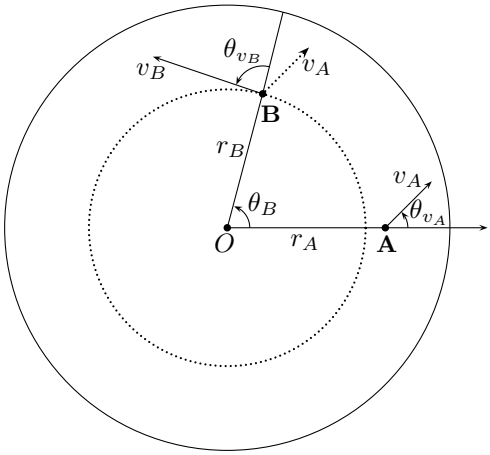

Fig. 3. Uniformity of Relative Movement Angle Distribution of Mobile Nodes

$$\theta_{v_{AB}} = \theta_B + \theta_{v_B} - \theta_{v_A} \tag{7}$$

where $\theta_{v_{AB}}$ is the relative angle from v_A to v_B.

Let us further assume that $f_R(r)$ is the PDF of node distribution, denoting the probability density that a node is found at a distance r from O. Also, let $f_{\Theta_V}(\theta_v|\mathbf{P} = \mathbf{p})$ denote the PDF of movement direction of a node at location $\mathbf{p}$, where the movement direction is calculated from the line $O\mathbf{p}$. Due to rotational symmetry of circular region, we can make the following statements without any calculation. First, given that a node is located at r distance away from the pole, the angle coordinate of node B from the polar axis is uniformly distributed, that is:

$$f_{\Theta_B}(\theta_B|r) = \frac{1}{2\pi}, \quad \theta \in [0, 2\pi)$$

Second, the movement angle distribution of a node at a position $\mathbf{p} = (r, \theta)$ is only dependent on r. That is,

$$f_{\Theta_V}(\theta_v|\mathbf{P} = \mathbf{p}) = f_{\Theta_V}(\theta_v|r_{\mathbf{p}} = r)$$

Given r_A, θ_{v_A}, r_B, and θ_{v_B}, the conditional PDF of relative movement angle distribution, $f_{\Theta_{V_{AB}}}(\theta_{v_{AB}})$, is given as

$$\begin{aligned} f_{\Theta_{V_{AB}}}(\theta_{v_{AB}}|r_A, \theta_{v_A}, r_B, \theta_{v_B}) &= f_{\theta_B}(\theta_B + \theta_{v_B} - \theta_{v_A}) \\ &= \frac{1}{2\pi} \end{aligned} \tag{8}$$

That is, given a pair of values for θ_{v_A} and θ_{v_B}, for any value of $\theta_{v_{AB}}$ there exists a value from uniformly distributed θ_B that satisfies the relationship given by Equation (7).

The unconditional PDF, $f_{\Theta_{V_{AB}}}(\theta_{v_{AB}})$, is given as

$$\begin{aligned} f_{\Theta_{V_{AB}}}(\theta_{v_{AB}}) &= \int_0^a \int_0^{2\pi} \int_0^a \int_0^{2\pi} f_R(r_A) f_{\Theta_V}(\theta_{v_A}|r_A) f_R(r_B) \times \\ & f_{\Theta_V}(\theta_{v_B}|r_B) f_{\Theta_{V_{AB}}}(\theta_{v_{AB}}|r_A, \theta_{v_A}, r_B, \theta_{v_B}) d\theta_{v_B} dr_B d\theta_{v_A} dr_A \\ &= \frac{1}{2\pi} \int_0^a \int_0^{2\pi} \int_0^a \int_0^{2\pi} f_R(r_A) f_{\Theta_V}(\theta_{v_A}|r_A) \times \\ & \quad f_R(r_B) f_{\Theta_V}(\theta_{v_B}|r_B) d\theta_{v_B} dr_B d\theta_{v_A} dr_A \\ &= \frac{1}{2\pi} \end{aligned} \tag{9}$$

The final result is obtained as each integral integrates a PDF and evaluates to 1. This gives the required proof. ■

We can see that independent of the PDF of node distribution, $f_R(r)$, and the PDF of movement angle distribution, $f_{\Theta_V}(\theta_v)$, the uniformity of relative movement angles holds in a circular region. That is, although Bettstetter et al. [2] shows that movement direction of a single mobile node has a strong bias towards the center, the relative movement direction of two mobile nodes is uniform in a circular area due to rotational symmetry. For simplicity, we also assume that the relative movement angle distribution is approximately uniform in a square region.

Now let us discuss the inter-contact time among mobile nodes. Let $f(x, y)$ denote the stationary node distribution PDF at location (x, y), then the PDF of node distribution for node N at location (x, y) is given by $f(x, y)$. And, following Equation (5), the probability, $p(x, y)$, of node M meeting node N at $X(x, y)$ in one epoch is given by

$$p(x, y) = 2r\bar{L}f^2(x, y)$$

The unconditional probability, P_U, for area $\mathcal{A}$ is given by

$$P_U = \iint 2r\bar{L}f^2(x, y)dxdy = \lambda\bar{T}$$

where $\lambda = 2\rho r\tilde{v}/A$, in which $\rho = A \iint f^2(x, y)dxdy$ and $\tilde{v}$ is the relative speed of M and N,

Following similar arguments for the static location case, the approximated CDF of inter-contact times is approximated as follows:

$$F(t) = 1 - e^{-\lambda t} \tag{10}$$

where $\lambda = 2\rho r\tilde{v}/A$.

Similar analytical results are presented in [14]. However, the exponentiality of inter-contact times is explained by assuming that the node movement for an arbitrarily small interval is independent of previous movement. This assumption is not valid in epoch-based movement models, as the node must complete an epoch before it can choose a new movement direction and movement speed.

3) Calculation of ρ for Random Waypoint Model: In RWP model, the value of ρ depends on the shape of $\mathcal{A}$, and can be calculated analytically or numerically when $f(x, y)$ is known. For the square area, approximate values of ρ for be calculated as 1.3683 [13][1].

[1]This value is calculated in [13] based on analytical results from [20]. However, note that numerically calculating ρ according to analytical results from [3] gives 1.3805.

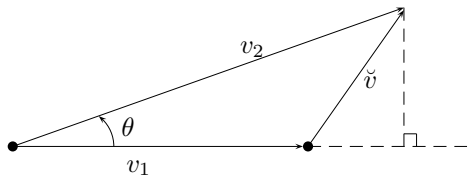

Fig. 4. Relative Speed of Two Mobile Nodes

To calculate the ρ value of the circular region, we consider a unit disk of size π. From the polynomial approximations of the PDF of node distribution given by [20] for unit disk, we use the following:

$$P(r) = \frac{3(1 - r^2)(189 - 44r^2 - 18r^4)}{257\pi}$$

With this function, we calculate the value of ρ as follows:

$$\begin{aligned} \rho &= A \iint_{\mathcal{A}} f^2(x, y)dxdy \\ &\approx \pi \int_0^{2\pi} \int_0^1 P^2(r)rdrd\phi \\ &= 18\pi^2 \int_0^1 \frac{r(1 - r^2)^2(189 - 44r^2 - 18r^4)^2}{(257\pi)^2} dr \\ &= \frac{3272289}{2311715} \\ &\approx 1.4155 \end{aligned}$$

4) Expected Relative Speed under Random Waypoint Model: The expected speed of a single node under RWP model is given as below [33]:

$$\bar{v} = \frac{\bar{L}}{\bar{T}} = \frac{v_{max} - v_{min}}{\ln(v_{max}/v_{min})}$$

This is due to the fact that the time a node spends at speed v is inversely proportional to v in RWP model. The PDF, $f_V(v)$, of a node's speed under RWP model is given as follows [7, 14]

$$f_V(v) = \frac{1}{v \ln(\frac{v_{max}}{v_{min}})}$$

The expected relative speed of two mobile nodes is given by

$$\begin{aligned} \tilde{v} &= \int_{v_{min}}^{v_{max}} \int_{v_{min}}^{v_{max}} \int_0^{2\pi} f_V(v_1) f_V(v_2) f_\Theta(\theta) \breve{v} d\theta dv_2 dv_1 \\ &= \frac{1}{2\pi \ln^2(\frac{v_{max}}{v_{min}})} \int_{v_{min}}^{v_{max}} \int_{v_{min}}^{v_{max}} \int_0^{2\pi} \\ & \quad \frac{\sqrt{(v_2 \sin\theta)^2 + (v_1 - v_2 \cos\theta)^2}}{v_1 v_2} d\theta dv_2 dv_1 \end{aligned} \tag{11}$$

where θ is the relative angle between $\overrightarrow{v}_1$ and $\overrightarrow{v}_2$, measured counter-clockwise from the direction of $\overrightarrow{v}_1$, and the instantaneous relative speed is denoted as $\breve{v}$, as shown in Figure 4. As given in Theorem 4, we take that θ is uniformly distributed.

We can see from (11) above that for different pairs of v_{min} and v_{max} that give the same $\bar{v}$, the expected relative speed may vary. That is, knowing $\bar{v}$ is not sufficient to obtain the relative speed, $\tilde{v}$, without taking the distribution of the speed into account. Under the simplifying condition that $v_{min} = v_{max} = \bar{v}$ or $v_{min}/v_{max} \approx 1$, the relative speed can be given as follows:

$$\begin{aligned}\tilde{v} &= \frac{\bar{v}}{2\pi}\int_0^{2\pi}\sqrt{\sin^2\theta + (1-\cos\theta)^2}d\theta \\ &= \frac{\bar{v}}{2\pi}\int_0^{2\pi}\sqrt{2(1-\cos\theta)}d\theta \\ &\quad [\text{substitution: } \cos\theta = \cos^2(\theta/2) - \sin^2(\theta/2)] \\ &= \frac{\bar{v}}{\pi}\int_0^{2\pi}\Big|\sin\frac{\theta}{2}\Big|d\theta \\ &= \frac{4\bar{v}}{\pi} \qquad (12)\end{aligned}$$

where θ is the angle between two movement directions.

C. Inter-contact Times in Random Direction Model

Compared to the RWP model, the node distribution in RD model is uniform: $f(x,y) = 1/A$ [4][22], and the average speed is simply given as $\bar{v} = (v_{max} + v_{min})/2$. When the epoch length is small compared to average inter-contact time, we can follow the analysis for RWP and show that the inter-contact times are exponentially distributed, where the CDF approximation is given as

$$F(t) = 1 - e^{-\lambda t}$$

where $\lambda = 2r\bar{v}/A$.

When two nodes move according the RD model, the CDF for inter-contact time is approximated as

$$F(t) = 1 - e^{-\lambda t} \qquad (13)$$

where $\lambda = 2r\tilde{v}/A$. Here $\tilde{v}$ is the relative speed of two nodes under RD model, which can be given as follows:

$$\begin{aligned}\tilde{v} &= \frac{1}{2\pi(v_{max}-v_{min})^2}\int_{v_{min}}^{v_{max}}\int_{v_{min}}^{v_{max}}\int_0^{2\pi} \\ &\quad \sqrt{(v_2\sin\theta)^2 + (v_1 - v_2\cos\theta)^2}d\theta dv_2 dv_1 \qquad (14)\end{aligned}$$

where θ is the relative angle between $\overrightarrow{v}_1$ and $\overrightarrow{v}_2$, measured counter-clockwise from the direction of $\overrightarrow{v}_1$.

The results for $\tilde{v}$ under RD model when $v_{max} = v_{min}$ or $v_{max}/v_{min} \approx 1$ is the same with RWP model as given in (12).

D. Summary

We can see our result for inter-contact rate for RWP is different from the result for meeting times given in [31], where the difference of inter-contact rates among mobile nodes under RWP and RD models is attributed to relative speed on the account that the relative movement angle is not uniform under RWP model. With Theorem 4 we see that the relative movement angle can also be considered uniform under RWP, and that the difference in inter-contact rates under these two models is a combined result of non-uniform node distribution under RWP as explained by factor ρ and the differences in the calculation of the relative movement speed for RWP and RD models, as shown by Equations (11) and (14), respectively.

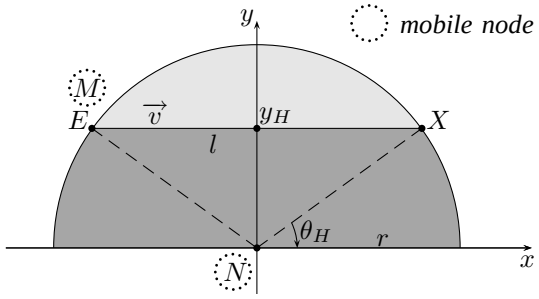

Fig. 5. Calculation of Observed Arrival Rate

IV. The Effect of Beaconing on Inter-contact Rate

In this section, we consider more realistic modeling of mobility by considering the effect of using beacon messages on inter-contact rate.

In the analysis in the previous section, we assumed that when a mobile node enters within the range of another node it is immediately sensed. In practical application scenarios, however, nodes announce their presence by broadcasting $HELLO$ or *beacon* messages at regular intervals, and a node may not be sensed if it finishes crossing the radio circle of another node before it sends a $HELLO$ message. Other factors such as transmission errors, channel contention, etc., can also cause nodes to miss $HELLO$ messages. Under such circumstances, the observed inter-contact rate will be different than the inter-contact rates discussed earlier in this section. Here we focus on the effect of $HELLO$ interval on the observed rate of inter-contact times.

We first define the expected distance covered by the mobile node within two hello messages as $HELLO$ *Distance*, L_H, as $L_H = T_H * \bar{v}$, where T_H is the $HELLO$ interval and $\bar{v}$ is the average speed ($\tilde{v}$ is used when both nodes are mobile). For practical purposes we assume that $0 < L_H < 2r$.

Theorem 5: Let λ denote the theoretical inter-contact rate, the observed inter-contact rate, λ', is given as

$$\lambda' = \lambda(\sin\theta_H + \frac{\pi - 2\theta_H - \sin 2\theta_H}{4\cos\theta_H})$$

where $\theta_H = arccos(L_H/2r)$.

Proof: Let us consider Figure 5 for our analysis of observed inter-contact rates, where a mobile node M crosses the radio range of N. We denote the distance covered within the circle, $\|EX\|$, as l. Let us use y_H to denote the value of y when $L_H = l$, and use θ_H for the corresponding θ angle. It is easy to see that in the heavily shaded region below y_H, node M will be detected with probability 1, whereas in the lightly shaded area the probability will be less than 1. Formally, the probability, P_d, that the node will be detected while crossing

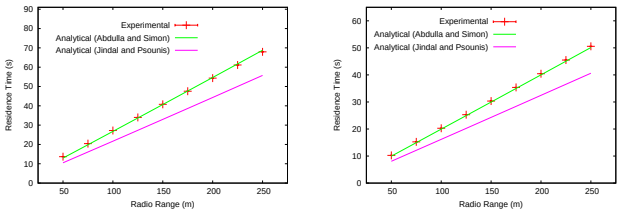

(a) Static Nodes (b) Mobile Nodes

Fig. 6. Contact Times

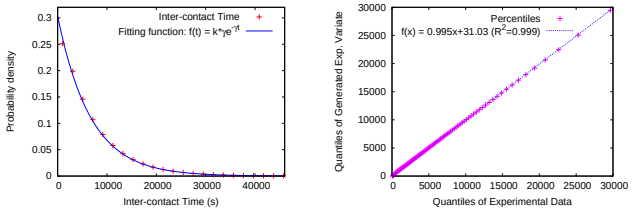

(a) Histogram of Inter-contact Times (b) Linear Regression Analysis

Fig. 7. Exponentiality of Inter-contact Times

the radio circle can be given as follows as a function of the intersection point y:

$$P_d(y) = \begin{cases} \frac{\sqrt{r^2-y^2}}{r\cos\theta_H}, & y_H < y < r \\ 1, & 0 \le y \le y_H \end{cases}$$

Due to symmetry we only consider the semicircle where $0 \le y$. It is easy to see that $\theta_H = arccos(L_H/2r)$ and that $y_H = r\sin\theta_H$.

The expected probability of node M being detected by N can be expressed as follows:

$$\begin{aligned} P_d &= \frac{1}{r}\int_0^r P_d(y)dy \\ &= \frac{1}{r}\int_0^{y_H} P_d(y)dy + \frac{1}{r}\int_{y_H}^r \frac{\sqrt{r^2-y^2}}{r\cos\theta_H}dy \\ &= \sin\theta_H + \frac{\pi - 2\theta_H - \sin 2\theta_H}{4\cos\theta_H} \end{aligned} \quad (15)$$

Applying P_d in relationship $\lambda' = P_d\lambda$ gives the required proof. ■

As expected, we notice that observed rate of inter-contact decrease as we increase the $HELLO$ interval.

V. Experimental Results

In this section, we present experimental results for mobility characteristics. The goal of our experiments is to verify the correctness of analytical results regarding contact times, relative movement angle, relative speed, and inter-contact times.

A. Experimental Settings

Most of our experiments use the ns-2 network simulator extended with our own code. We also use our custom simulator for experiments in circular areas, as well as for detailed measurements of the relative speed and movement angles.

The default settings for ns-2 simulations are as follows. Each simulation run has 40 nodes moving according to the specified mobility model in a $6000m \times 6000m$ square area. By default, nodes have a radio range of $250m$. Minimum and maximum speeds, v_{min} and v_{max}, are $3m/s$ and $10m/s$, respectively. The $HELLO$ interval is set to 3 seconds.

To measure contact and inter-contact times, a node stores the time when another node is found in its radio range for the first time. When a $HELLO$ message is not heard within a $HELLO$ interval (plus a small tolerance time), the node is marked as gone out of radio range and the contact time is recorded as the time elapsed. Inter-contact time is recorded when it receives a $HELLO$ message again from the destination. The process repeats in this manner. For the relative speed and relative movement angles, we use our custom simulator, and calculate the relative speed and relative movement angles of a pair of nodes at every 0.1 second. We ran each experiment 29 times with random seeds. Data points presented are plotted with 95% confidence intervals.

For Random Waypoint with hot-spots, we also use our custom simulator for the measurement of inter-contact times of a pair of mobile nodes, A and B, moving in a square area of size $6000m \times 6000m$. A square region of width $500m$ is designated as the hot-spot for A. The coordinate of the square hot-spot is set at $(1500, 1500)$. A square region of the same size is placed at $(4500, 4500)$ as a hot-spot for node B. To obtain the inter-contact time characteristics shown in our experimental results, for each mobile node the probability of choosing its hot-spot as its next waypoint is varied between 0.7-0.8, and the pause time inside the hot-spot is set to $300s$ and the pause time outside the hot-spot is set to $3s$.

B. Mobility Characteristics

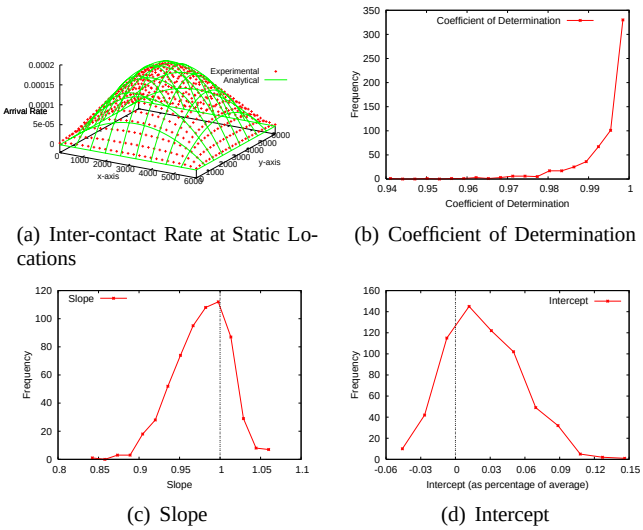

(a) Inter-contact Rate at Static Locations (b) Coefficient of Determination

(c) Slope (d) Intercept

Fig. 8. Linear Regression Analysis for the Exponentiality of Inter-contact Times

Below we discuss the simulation results for contact times and inter-contact times for static locations as well as for cases

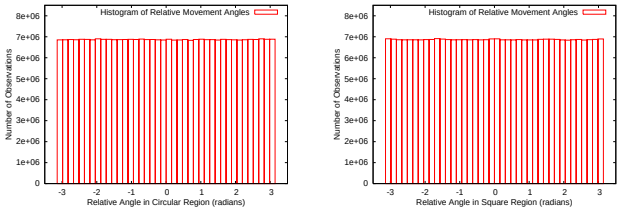

(a) Circular Region (b) Square Region

Fig. 9. Relative Movement Angle Distribution

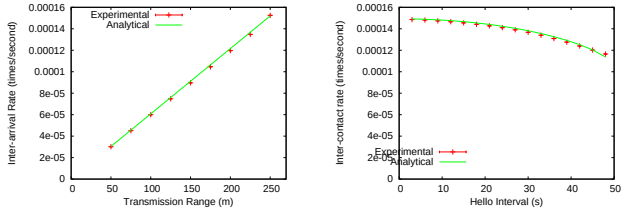

(a) Transmission range (b) Hello interval

Fig. 10. Effects of Transmission Range and Hello Interval on Inter-contact Rate

TABLE I
RELATIVE SPEED OF MOBILE NODES UNDER RANDOM WAYPOINT MODEL

Speed Settings			Analytical		Empirical	
v_{min}	v_{max}	$\bar{v}$	$\tilde{v}$	$\hat{v}$	$\tilde{v}$ (95% Conf. Int.)	$\hat{v}$
1	22.93	7	10.726	1.532	10.72 ($\pm$ 0.0034)	1.53
2	16.97	7	9.077	1.439	10.08 ($\pm$ 0.0029)	1.44
3	13.56	7	9.642	1.377	9.64 ($\pm$ 0.0026)	1.38
4	11.22	7	9.331	1.333	9.33 ($\pm$ 0.0018)	1.33
5	9.47	7	9.108	1.301	9.10 ($\pm$ 0.0020)	1.30
6	8.11	7	8.972	1.281	8.97 ($\pm$ 0.0020)	1.28
7	7	7	8.913	1.273	8.91 ($\pm$ 0.0020)	1.27

where both nodes are mobile. For this purpose, we place static nodes on a 25×25 grid, where neighboring nodes are $250m$ apart, for a total of 625 static nodes. These static nodes only listen to $HELLO$ messages sent by mobile nodes, and record contact times and inter-contact times. Mobile nodes also record the same statistics among each other.

1) Contact Times: Figure 6 shows the experimental and analytical results for contact times at static locations and among mobile nodes under RWP model. Analytical results for these two metrics are calculated according to (4) by using the average speed and the average relative speed, respectively. We can see that our analysis closely approximates the experimental results. We also obtain similar results for the Random Direction model.

2) Relative Velocity of Mobile Nodes: Figure 9 shows the histograms of relative movement angles of nodes moving according to the RWP model in circular and square regions. We can see that the distribution is virtually uniform for both areas, confirming Theorem 4.

Table I shows the effect of the distribution of v_{min} and v_{max} on relative speed, $\tilde{v}$. For this, we choose seven pairs of v_{min} and v_{max} that produce the same node average speed, $\bar{v} = 7$. To see the effects, we define normalized speed $\hat{v}$ as $\hat{v} = \tilde{v}/\bar{v}$. We can see that $\hat{v}$ changes as the distribution of minimum and maximum speeds, and that empirical results confirms the results given in Equation (11).

3) Inter-contact Times: We first look at inter-contact times among mobile nodes. Figure 7(a) shows the histogram of inter-contact times under Random Waypoint model. To test the exponentiality of inter-contact times, we perform linear regression analysis on the Quantile-Quantile (Q-Q) plot of two data sets: recorded inter-contact times and randomly generated exponential variates with the same average as that of the experimental data. For linear regression, we consider

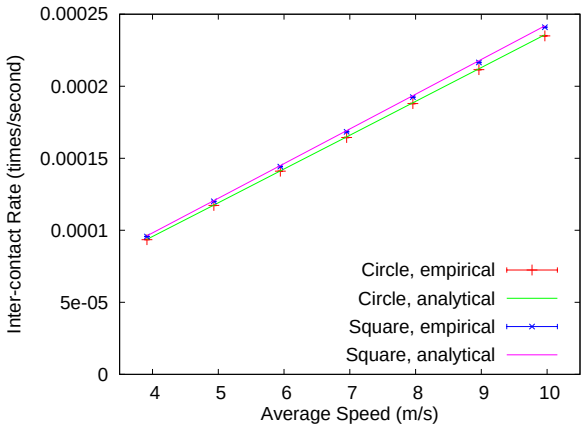

Fig. 11. Inter-contact Rates in Square and Circular Areas under Varying Speed

three factors: coefficient of determination (R^2), slope a, and intercept b. As shown in Figure 7(b), the recorded inter-contact times closely match the exponentially generated variates, with $R^2 = 0.999$, $a = 0.995$, and $b = 31.03$ (0.5% of average).

Under RWP model, inter-contact rates at specific locations depend on the PDF of node distribution. Figure 8(a) shows the average inter-contact rates observed by 625 static nodes. For each static location, we run similar linear regression analysis as described above for mobile nodes. Overall statistics for regarding R^2 values, slopes, and intercepts are shown in Figures 8(b)–8(d). We can see that exponentiality of inter-contact times strongly holds at static locations. We also identify that most of the deviations are due to border effects.

The effects of transmission range and $HELLO$ interval on the inter-contact rate is shown in Figure 10(a) and 10(b), respectively. These experimental results conform to analytical values that we obtain from (10) and (15).

Figure 11 shows the experimental and analytical results for inter-contact rates under varying speed in square and circular areas of the same size. As can be seen, Equation (10) with different ρ values accurately explains differences.

Although it has been shown that the inter-contact times can be very closely approximated as exponential under our experimental settings, a more detailed look show that inter-contact times differ from exponential distribution for smaller inter-contact times as depicted in Figure 12, where the number of bins used to get the histogram of inter-contact times is

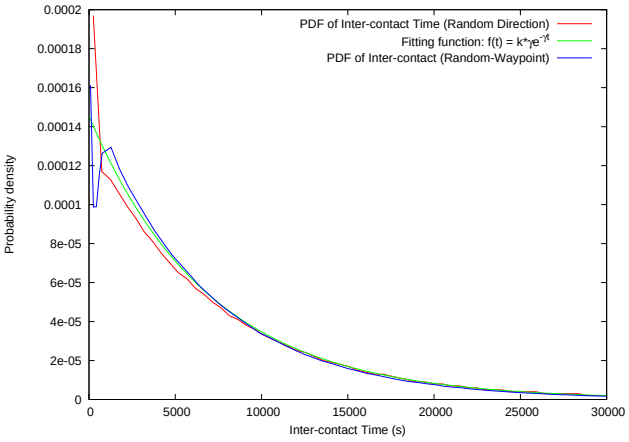

Fig. 12. Inter-contact Rates of Random Waypoint and Random Direction Model Compared to Exponential Distribution

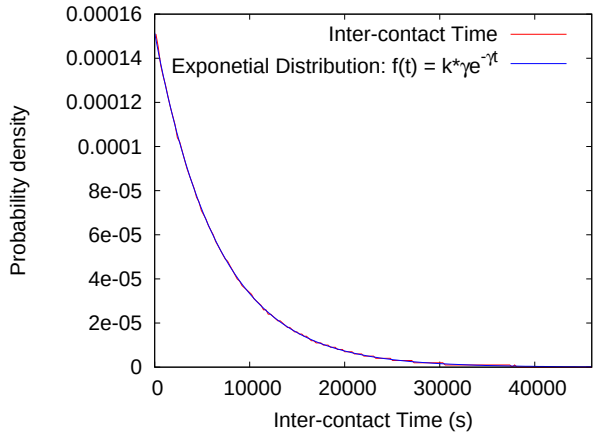

Fig. 13. Distribution of Inter-contact Times (larger than $1.5 * \bar{T}$) of RWP Model Compared to Exponential Distribution

increased to 200, as opposed to 40 used in Figure 7(a). We can see that for inter-contact times less than 3000 seconds, the inter-contact time distributions of both Random Waypoint and Random Direction differ from exponential distribution in different ways. This shows that although exponentiality assumption holds for both mobility models, such differences should be considered for simulations that assume that the inter-contact times are strictly exponential, especially for small inter-contact times.

VI. Conclusions

In this paper, we studied the properties of two commonly-used mobility models: Random Waypoint and Random Direction. We showed analytically that the inter-contact times of nodes can be approximated by the exponential distribution in these models under typical opportunistic network settings. We also provided analytical results for contact time, inter-contact time, effect of $HELLO$ intervals on inter-contact rate. Through extensive simulation study, we showed that our analytical results for mobility characteristics are accurate.

References

[1] F. Bai, N. Sadagopan, and A. Helmy. The IMPORTANT framework for analyzing the impact of mobility on performance of routing protocols for adhoc networks. INFOCOM, 2003.

[2] C. Bettstetter, H. Hartenstein, and X. Pérez-Costa. Stochastic properties of the random waypoint mobility model: Epoch length, direction distribution and cell change rate. In *MSWIM '02*. ACM Press, 2002.

[3] C. Bettstetter, G. Resta, and P. Santi. The node distribution of the random waypoint mobility model for wireless ad hoc networks. *IEEE Trans. on Mobile Computing*, 02(3):257–269, 2003.

[4] Christian Bettstetter. Mobility modeling in wireless networks: Categorization, smooth movement, and border effects. *ACM Mobile Computing and Communications Review*, 5(6):55–67, July 2001.

[5] Christian Bettstetter. Smooth is better than sharp: a random mobility model for simulation of wireless networks. In *MSWIM '01*, 2001.

[6] J. Le Boudec and M. Vojnovi. Perfect simulation and stationarity of a class of mobility models. INFOCOM, May 2005.

[7] Jean-Yves Le Boudec. Understanding the simulation of mobility models with palm calculus. Technical Report IC/2005/33, EPFL, 2005.

[8] A. Chaintreau, P. Hui, J. Crowcroft, C. Diot, R. Gass, and J. Scott. Impact of human mobility on the design of opportunistic forwarding algorithms. In *INFOCOM*, pages 1–13, April 2006.

[9] A. Jardosh et. al. Towards realistic mobility models for mobile ad hoc networks. In *MobiCom '03*, New York, NY, USA, 2003. ACM Press.

[10] X. Hong et. al. A group mobility model for ad hoc wireless networks. In *MSWiM '99*, pages 53–60, New York, NY, USA, 1999. ACM Press.

[11] Kevin Fall. A delay-tolerant network architecture for challenged internets. Karlsruhe, Germany, August 2003. ACM SIGCOMM'03.

[12] M. Garetto and E. Leonardi. Analysis of random mobility models with PDEs. In *MobiHoc '06*, pages 73–84, 2006.

[13] R. Groenevelt, P. Nain, and G. Koole. The message delay in mobile ad hoc networks. In *Performance*, 2005.

[14] Robin Groenevelt. *Stochastic Models for Mobile Ad Hoc Networks*. PhD thesis, INRIA Sophia Antipolis, 2005.

[15] Sushant Jain, Kevin Fall, and Rabin Patra. Routing in a delay tolerant network. ACM SIGCOMM'04, August 2004.

[16] Apoorva Jindal and Konstantinos Psounis. Fundamental mobility properties for realistic performance analysis of intermittently connected mobile networks. In *International Workshop on Intermittently Connected Mobile Ad hoc Networks*, pages 59–64, 2007.

[17] D. Johnson. Dynamic source routing in ad hoc wireless networks. *Wireless Networks*, 1995.

[18] Evan P. C. Jones, Lily Li, and Paul A. S. Ward. Practical routing in delay-tolerant networks. In *WDTN '05: Proceeding of the 2005 ACM SIGCOMM workshop on Delay-tolerant networking*, pages 237–243. ACM, 2005.

[19] T. Karagiannis, J.-Y. Le Boudec, and M. Vojnovic. Power law and exponential decay of inter contact times between mobile devices. Technical Report MSR-TR-2007, Microsoft Research, March 2007.

[20] Pasi Lassila. Spatial node distribution of the random waypoint mobility model with applications. *IEEE Transactions on Mobile Computing*, 5(6):680–694, 2006.

[21] J. Lee and J. Hou. Modeling steady-state and transient behaviors of user mobility:: formulation, analysis, and application. In *MobiHoc*, 2006.

[22] P. Nain, D. Towsley, B. Liu, and Z. Liu. Properties of random direction models. In *Proc. IEEE Infocom '05*. ACM Press, March 2005.

[23] W. Navidi and T. Camp. Stationary distributions for the random waypoint mobility model. *IEEE Transactions on Mobile Computing*, 03(1):99–108, 2004.

[24] C. Perkins and P. Bhagwat. Routing over a multihop wireless network of mobile computers. *Mobile Computing*, 1996.

[25] C. Perkins and E. Royer. Ad hoc on-demand distance vector routing. *Proc. of the 2nd IEEE Workshop on Mobile Comp. Sys. and Appl.*, 1999.

[26] R. Shah, S. Roy, S. Jain, and W. Brunette. Data mules: Modeling a three-tier architecture for sparse sensor networks. IEEE SNPA, 2003.

[27] T. Small and Z. J. Haas. Resource and performance tradeoffs in delay-tolerant wireless networks. In *WDTN '05*, pages 260–267, 2005.

[28] A. Spuropoulos, K. Psounis, and C. Raghavendra. Multi-copy routing in intermittently connected mobile networks. Technical Report CENG-2004-12, USC, 2004.

[29] T. Spyropoulos, K. Psounis, and C. Raghavendra. Single-copy routing in intermittently connected mobile networks. In *Sensor and Ad Hoc Communications and Networks*, pages 235–244. IEEE, Oct 2004.

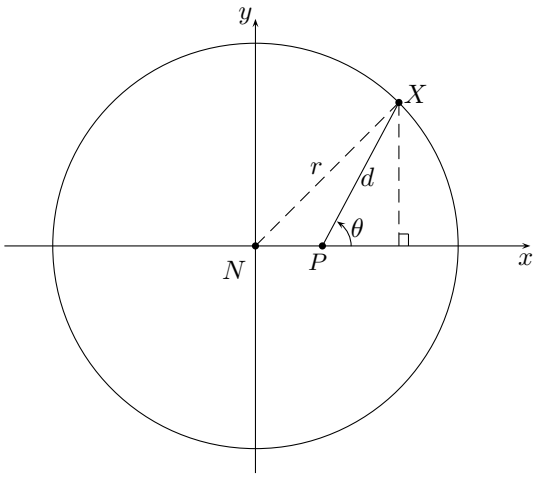

Fig. 14. Calculation of Contact Time

[30] T. Spyropoulos, K. Psounis, and C. Raghavendra. Spray and wait: An efficient routing scheme for intermittently connected mobile networks. Philadelphia, PA, USA, August 2005. ACM SIGCOMM'05 Workshops.
[31] T. Spyropoulos, K. Psounis, and C. Raghavendra. Performance analysis of mobility-assisted routing. pages 49–60. ACM Mobihoc 2006, 2006.
[32] M. M. Bin Tariq, M. Ammar, and E. Zegura. Message ferry route design for sparse ad hoc networks with mobile nodes. In *MobiHoc*, 2006.
[33] J. Yoon, M. Liu, and B. Noble. Random waypoint considered harmful. *INFOCOM*, 2003.
[34] X. Zhang, G. Neglia, J. Kurose, and D. Towsley. Performance modeling of epidemic routing. Technical Report CMPSCI 2005-44, UMass, 2005.
[35] W. Zhao, M. Ammar, and E. Zegura. A message ferrying approach for data delivery in sparse mobile ad hoc networks. MobiHoc, May 2004.

APPENDIX

To find the expected distance covered by a mobile node, M, before exiting the radio range of static node N, let us consider the graph shown in Figure 14. For simplification, we take the direction from the location of N to the pause point, P, as the direction of x-axis. Let θ denote the angle of the new movement direction of M measured counter-clockwise from the direction of x-axis, and let d denote the distance covered before node M exits the radio circle at point X. Assuming that the x-coordinate of P is x_p, and the transmission radius is r, from trigonometric relations we can have:

$$\begin{aligned} r^2 &= (d\sin(\theta))^2 + (d\cos(\theta) + x_p)^2 \\ &= d^2 + 2dx_p\cos(\theta) + x_p^2 \\ &= d^2 + 2dx_p\cos(\theta) + x_p^2\cos(\theta)^2 + x_p^2\sin(\theta)^2 \\ &= (d + x_p\cos(\theta))^2 + x_p^2\sin(\theta)^2 \end{aligned}$$

Solving the equation above for d, we have

$$d = \sqrt{r^2 - x_p^2\sin(\theta)^2} - x_p\cos(\theta)$$

Without any particular assumption regarding the original movement direction of M and the location of N, we assume that θ is uniformly distributed and give the following expression for the expected distance, $\bar{d}$,

$$\begin{aligned} \bar{d} &= \frac{1}{2\pi r}\int_0^r\int_0^{2\pi}\left(\sqrt{r^2 - x_p^2\sin(\theta)^2} - x_p\cos(\theta)\right)d\theta dx_p \\ &= \frac{1}{2\pi r} * r\int_0^r\int_0^{2\pi}\sqrt{1 - \left(\frac{x_p}{r}\right)^2\sin(\theta)^2}\,d\theta dx_p \\ &= \frac{1}{2\pi}\int_0^r \mathrm{E}\left(2\pi|\left(\frac{x_p}{r}\right)^2\right)dx_p \\ &\quad (\text{change of variable: } z = x_p/r) \\ &= \frac{r}{2\pi}\int_0^1 \mathrm{E}\left(2\pi|z^2\right)dz \\ &= \frac{r}{2\pi} * 2\pi * {}_3F_2\left(-\frac{1}{2}, \frac{1}{2}, \frac{1}{2}; 1, \frac{3}{2}; 1\right) \\ &\approx 0.901r \end{aligned}$$

where E is the incomplete elliptic integral of the second kind, and ${}_3F_2$ denotes hypergeometric series.